FALSE INDICATORS TO ACOUSTIC-TO-SEISMIC BURIED LANDMINE DETECTION
FINAL TECHNICAL REPORT
GRANT NUMBER: N00014-02-1-0878

SUBMITTED TO:

US OFFICE OF NAVAL RESEARCH
800 NORTH QUINCY STREET
ARLINGTON, VA 22217-5660

by

James M. Sabatier
National Center for Physical Acoustics
University of Mississippi
University, MS 38677

NCPA Report JS1107-01

28 NOVEMBER 2007

SECURITY CLASSIFICATION: UNCLASSIFIED

REPORT DOCUMENTATION PAGE

Form Approved
OMB No. 0704-0188

1. REPORT DATE *(DD-MM-YYYY)*	2. REPORT TYPE	3. DATES COVERED *(From - To)*
19-12-2007	Final Technical Report	1 Jul 2002-30 Sep 2007

4. TITLE AND SUBTITLE
False Indicators to Acoustic-to-Seismic Buried Landmine Detection

5a. CONTRACT NUMBER

5b. GRANT NUMBER
N00014-02-1-0878

5c. PROGRAM ELEMENT NUMBER

6. AUTHOR(S)
James M. Sabatier

5d. PROJECT NUMBER

5e. TASK NUMBER

5f. WORK UNIT NUMBER

7. PERFORMING ORGANIZATION NAME(S) AND ADDRESS(ES)
University of Mississippi
National Center for Physical Acoustics
PO Box 1848
University, MS 38677

8. PERFORMING ORGANIZATION REPORT NUMBER
JMS1207-01

9. SPONSORING/MONITORING AGENCY NAME(S) AND ADDRESS(ES)
Office of Naval Research
ONR Code 30
875 North Randolph Street
Arlington, VA 22203-1995

10. SPONSOR/MONITOR'S ACRONYM(S)
ONR Code 30

11. SPONSOR/MONITOR'S REPORT NUMBER(S)

12. DISTRIBUTION/AVAILABILITY STATEMENT
DISTRIBUTION STATEMENT A: Approved for public release. Distribution unlimited.

13. SUPPLEMENTARY NOTES

14. ABSTRACT
The proliferation of relatively cheap landmines in many of the world's conflicts has led to a critical situation. Most methods of locating landmines trigger on too many false alarms must each be investigated before declaring an area to be clear of mines. This led to the need for an accurate means of detection coupled with a low false alarm rate. The University of Mississippi has developed an acoustic/seismic technique to meet this need. In 2002, the Office of Naval Research issued Grant N00014-02-1-0878 to conduct research to better understand the causes of false alarms using this method and to develop methods to significantly reduce them. This report discusses the significant research advances including a clearer understanding of the phenomenology underlying the technology, development of models, and signal processing techniques to reduce false alarms.

15. SUBJECT TERMS
Landmine detection, false alarms, acoustic-to-seismic

16. SECURITY CLASSIFICATION OF:			17. LIMITATION OF ABSTRACT	18. NUMBER OF PAGES	19a. NAME OF RESPONSIBLE PERSON
a. REPORT	b. ABSTRACT	c. THIS PAGE			Eric Freimark
					19b. TELEPHONE NUMBER *(Include area code)*
U	U	U	SAR	28	662-915-1556

FALSE INDICATORS TO ACOUSTIC-TO-SEISMIC BURIED LANDMINE DETECTION

0.0 ABSTRACT

The U. S. Office of Naval Research (ONR) issued Grant N00014-02-1-0878 24 for False Indicators to Acoustic-to-Seismic Buried Landmine Detection to the National Center for Physical Acoustics (NCPA) at the University of Mississippi. This report covers the period from 1 July 2002 through 30 September 2007. Significant advances were made in the understanding of the causes of false alarms for the acoustic mine detection technology during this grant. These advances include a clearer understanding of the phenomena underlying the technology, development of models, and development of signal processing techniques to reduce false alarms.

The key results of this research were published in scientific journals and in graduate theses/dissertations. Peer-reviewed publications include:

- V. N. Fokin, M. S. Fokina, J. M. Sabatier, N. Xiang, and W. B Howard, "Effect of variability of soil physical properties on clutter and false alarms in landmine detection," Radio Sci., 39, RS4S04 (2004)
- Vladimir N. Fokin, Margarita S. Fokina, James M. Sabatier, and Zhiqu Lu, "Effect of ground variability on acoustic-to-seismic transfer function and false alarms in landmine detection," J. Acoust. Soc. Am., 120(2), 621-630 (2006).
- D. Velea, R. Waxler, and J. M. Sabatier, "An effective fluid model for landmine detection using acoustic to seismic coupling," J. Acoust. Soc. Am., 115 (5), 1993-2002 (2004).
- W. C. Kirkpatrick Alberts II, James M Sabatier, Roger Waxler, "Resonance frequency shift saturation in acoustic landmine detection experiments," J. Acoust. Soc. Am. 120(4), 1881-1886 (2006)
- W. C. Kirkpatrick Alberts II, Roger Waxler, and James M Sabatier, "Studying the mechanical behavior of a plastic, shock-resisting, anti-tank landmine," J. Acoust. Soc. Am. 120(6), 3655-3663 (2006).

Graduate degrees completed as part of this program included:

- Doctoral dissertation completed: W. C. K. Alberts II, "A study of the acoustic behavior of a plastic blast hardened antitank landmine," University of Mississippi, October 2005.
- Master's thesis completed: G. Matalkah, "Apparatus and algorithms for acoustic landmine detection," University of Mississippi, May 2007.

1.0 TABLE OF CONTENTS

0.0 Abstract	2
1.0 Table of Contents	3
2.0 Introduction	3
3.0 Methods, Assumptions, and Procedures	3
4.0 Results and Discussion	5
5.0 Bibliography	15
6.0 Graduate Students Supported	16
7.0 References	16
Appendices	
A. The Effect of Soil Reconsolidation on Acoustic Mine Detection	A-1

2.0 INTRODUCTION

The proliferation of relatively cheap landmines in many of the world's conflicts has led to a critical situation. Most methods of locating landmines trigger on too many false alarms that must each be investigated before declaring an area to be clear of mines. Meanwhile, plastic landmines have been developed that cannot be detected using metal detectors. The confluence of these two factors led the US Department of Defense to seek accurate means of detection coupled with a low false alarm rate. The Office of Naval Research (ONR), Army Research Office (ARO), and US Army Night Vision and Electronic Sensors Directorate (NVESD) issued a series of contracts and grants to the University of Mississippi's National Center for Physical Acoustics (NCPA) to demonstrate and advance the ability of acoustic/seismic techniques in locating landmines.

Using this technique, landmines are acoustically located by exciting the ground using sound or seismic waves. The mine, a hollow, man-made object, resonates, causing the insonified ground to vibrate with greater amplitude. The vibration is measured using a non-contact device, such as a laser Doppler vibrometer (LDV) and the signal is processed to produce an image of the buried landmine.

NCPA has demonstrated the effectiveness of this technique in testing under varying conditions at the University of Mississippi, Fort A. P. Hill VA, and Yuma Proving Grounds AZ. These tests have included blind tests in which the testers did not know whether or not a section of ground contained a mine and have included both downward and forward-looking tests. The results of each test series clearly showed that the acoustic technique is a very accurate means for locating landmines.

In 2002, ONR issued Grant N00014-02-1-0878 to NCPA to conduct research to better understand the causes of false alarms and to develop methods to significantly reduce them.

3.0 METHODS, ASSUMPTIONS, AND PROCEDURES

The physics underlying acoustic mine detection and the baseline methodology in use during this grant are discussed in detail in the Final Reports for Contracts DAAB07-97-C-6040 [1], DAAB15-00-C-1005 [2], and DAAB15-02-C-0024 [3]. The purpose of this grant was to better understand the causes of false alarms for acoustic/seismic mine detection and develop

methods to mitigate them. During this grant, many variations of equipment for acoustic/seismic landmine detection were in use and are described in Reference [3].

Generically speaking, energy radiates from an excitation source in the vicinity of the target area. The excitation source may be either loudspeakers or mechanical shakers. The energy couples into the ground and induces resonance in manmade objects such as landmines. The vibration of the ground surface is amplified by resonance in the buried objects. Mines are located by comparing the magnitude of the vibrational amplitude of the ground over the mines to the magnitude of the vibrational amplitude away from the mines. Areas of higher amplitude indicate possible mines. When mapped, if these areas of increased amplitude are the right size and shape for a mine, and are consistent over a number of frequency bands, then the decision is made that a mine is present. Figure 1 schematically illustrates the measurement setup employed in outdoor field measurements. Several configurations were used in field testing. Figure 2 shows a photograph of an acoustic-to-seismic landmine detection data collection apparatus used in field-testing early in the contract that employs a single-beam scanning LDV and loudspeakers. Figure 3 shows the functional prototype of the confirmation sensor currently used for landmine detection testing.

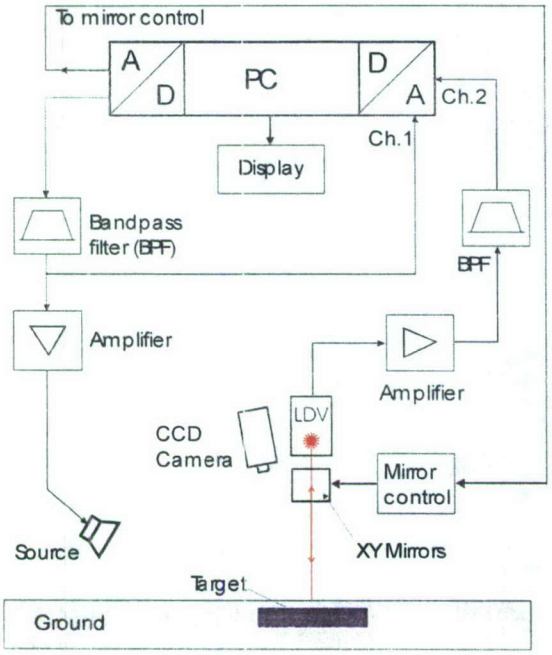

Figure 1. Schematic diagram of the measurement apparatus used in acoustic-to-seismic landmine detection.

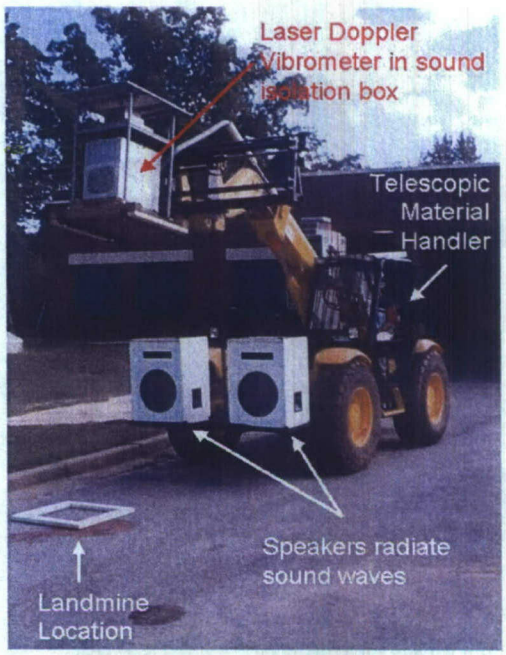

Figure 2. Photograph of the acoustic-to-seismic landmine detection data collection apparatus with a scanning single-beam LDV and loudspeakers.

Figure 3. Functional prototype of a confirmation sensor with mechanical shakers and multiple-beam vibrometer.

4.0 Results and Discussion

The research conducted under this grant fell under four basic tasks: (1) analysis of existing data to better understand clutter and strong false indicators; (2) identification of physical properties of the soil that cause the S/A ratio response associated with strong false indicators; (3) linear and nonlinear S/A-coupling experimentation to study strong false indicators; and (4) development of models used to predict and mitigate false alarms.

Soil Property Variations

One key source of false alarms lies in the variability of soil properties. Experimentation, data analysis and modeling have shown a strong influence of the spatial variability of ground properties on fluctuations in the acoustic-to-seismic transfer function (A/S TF), the ratio of the normal particle velocity on the ground to sound pressure. In some cases, these fluctuations may lead to false alarms in landmine detection.

To understand the effects of acoustic natural velocity variability and their influence on potential false indicators in landmine detection, the following research was performed.

Numerical investigations of the features of the acoustic-to-seismic transfer function in the vicinity of the critical angles

Computations of the acoustic-to-seismic transfer function (*TF*) for typical sets of soil parameters were performed with original code based on the Dunkin-Thrower's matrix approach. Numerical investigations show that in the vicinity of critical angles increased energy reflection from the deeper layers toward the air/soil interface resulting in an increase in the magnitude of the *TF* and lead to rapid changes in the phase of the *TF*. At the lower frequencies, the sound wavelength may be much greater than the thickness of the soil layer ($\lambda >> d$); the wave is not significantly affected by the thin layer. It was revealed that both critical angles that are connected with the layering of the ground and sound speeds in the half-space may be determined on the "frequency-angle" plane, when the frequency is sufficiently high. Comparison between measured and calculated transfer function was performed. It shows that layered viscoelastic

model of the ground may be successfully used for analysis of influence of ground parameters on the acoustic-to-seismic transfer function.

Effect of ground variability on the acoustic-seismic transfer function

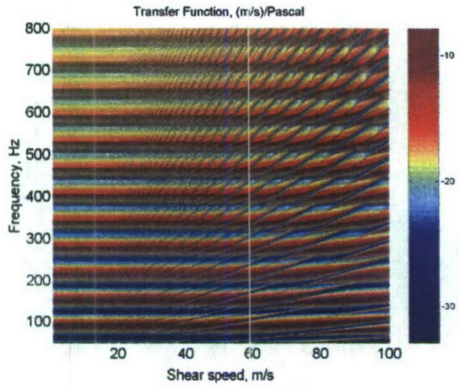

Figure 4

To understand the effect of natural variability of ground parameters on the acoustic-to-seismic *TF*, numerical investigations were performed for the model consisting of one elastic layer covering an elastic half space. Numerical investigations shown that density, attenuation of compressional and shear waves and parameters of the elastic half-space have less effect on the acoustic-to-seismic *TF* than the thickness, compressional and shear speed of the layer. Here we will consider only the effect of shear wave speed in the layer on the acoustic-to-seismic *TF*. It is convenient to examine the *TF* on the "frequency-shear speed" plane (Figure 4). All other parameters of the model are kept constant.

Minima and maxima of *TF* in Figure 4 form a set of the fan-like straight lines coming from the point with the coordinates (0,0). Analysis of $TF(f,c_t)$ make it possible to explain why the number of the false indicators increases when the frequency increases. For a 1 m^2 outdoor soil plot, let c_t has a range of 90-100 m/s variability from one spatial point to another. At low frequency range (f=50 Hz) changing of c_t does not lead to significant changes in the *TF*. A horizontal section at 50 Hz of the surface in Figure 4 shows that the value of *TF* doesn't significantly change for this range of shear speeds. However, in the high frequency range (f=800 Hz) the *TF* value changes from a maximum to a minimum twice within the same variation of c_t in the layer. This means that small variations of c_t will more probably cause fluctuations in the *TF* at high frequencies than at low frequencies. Therefore, the presence of natural ground variations of c_t will lead to an increase in the clutter level at higher frequencies when compared with lower frequencies for the same spot.

Effect of distributed sound sources on the transfer function

In the configurations used for landmine detection, the size of the sound source is comparable with the distance to the point of measurement. As a first approximation, the sound field at the point of measurement may be presented as a function of the source aperture over a range of corresponding incidence angles. Integration of the plane wave $TF(f,\theta)$ over the range of incidence angles will give $TF(f)$ for a distributed source. The positions of the *TF* maxima change slowly with changing of the angle, when $0^o<\theta<\theta_1$ and $\theta_2<\theta<90^o$, here $\theta_{1,2}=arcsin(c_0/c_{t,l})$ are critical angles. Analyzing the dependence of the transfer function as a function of angle, one may notice that integration by angle will have practically no effect on transfer function in the range of $\theta=0^o$-θ_1 and $\theta=\theta_2$-90^o. This influence may be dramatic if the range of integration of the *TF* includes angles between critical angles θ_1 and θ_2. In this case, peaks of the transfer function will be lower and wider than peaks of the *TF* for a single angle. This may be a reason why experimentally-measured transfer functions often have wider peaks than calculated ones. If the range of integration includes the critical angles, the positions of minima and maxima in the

integrated *TF* may be different from the positions of minima and maxima for average angle within the range of integration. Therefore, the *TF* for a distributed sound source always retains the main features that are connected with propagation of compressional and shear waves in the layered structure of the ground.

Experimental investigations and analysis of data to verify the ideas concerning clutter and strong false indicators

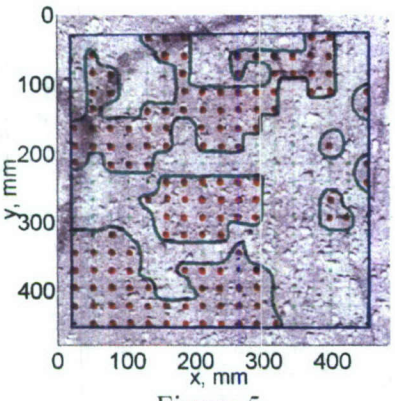

Figure 5

Experimental investigations using a high frequency resolution were performed on a dirt lane at an Army test site to understand the physical nature of the natural velocity variability and its influence on false indicators. At the time of measurements, the surface of the ground within the measurement site visually consisted of wet and dry spots of irregular shapes as seen in the background CCD camera photo (Figure 5). Positions of measurements points within the scan area with high particle velocities vary from one frequency sub-band to another and seem to have random locations. Analysis of LDV data revealed that measurement points with high particle velocity are co-located with the wet spots of the soil surface. Further, regions or sub-areas consisting of several near by measurement points with high normal velocities and the areas of the wet spots on the surface of the ground are visually, highly correlated. The result of combining the high velocity measurement points (red points) and the visual photo image of the scanned area is shown in Figure 5. The red points were accumulated in the frequency band 420-650 Hz. It is clearly seen that locations of the wet spots and the high velocity points are highly correlated.

A simple model was suggested to explain this phenomenon. Heavy equipment used in the construction of the road (graders and rollers) produced regions with different strain states due to inhomogeneity of the road material. Regions with higher strain states have greater densities and higher sound speeds. These regions will have lower water permeability and lower porosity and dry more quickly after rain than regions with lower strain states, less density and lower sound speeds. Numerical investigations show that a ground with low density and low sound speed has a higher magnitude of the *TF*. This explains the correlation between the regions with higher magnitude of *TF* and the wet regions. It is believed that spatial locations that have high particle velocity in different frequency sub-bands may be due to variation of the depth of the inhomogeneity of the layer within the wet regions. This model gives a physical understanding the nature of natural velocity variability and link between the physical properties of soil and magnitude of the acoustic-seismic transfer function.

Estimation of average properties of the ground

To investigate the false alarm rate, it is important to know both the average and local properties of the ground. A technique was developed to obtain the average properties of the ground and the approximate depth of the layers in the ground. The technique explores the horizontal waveguide properties of the top layer of the ground. Due to the layered structure of the ground, the acoustic waves may propagate in an undersurface waveguide forming the

structures on the frequency-range plane (Figure 6). Using a Fourier transform along the range axis, the dependencies of the wave numbers upon the frequency may be obtained (Figure 7). According to the mode theory, the asymptotes coming from the point (0,0) should exist on the wave number-frequency plane (dashed lines). From the inclinations of these asymptotes, the minimum and maximum sound speeds in the waveguide, which were equal to 100m/s and 530m/s respectively in this case, may be determined. To determine the depths of the layers, one may take the Fourier transform from the experimental field data along the frequency axis and reveal the time structure of the signal. The periods in the time delays are related to the depths of the layers in the ground. Consequently, it is possible to estimate the depths of the layers as well as to estimate the sound speed in the top layer of the ground. These estimations of the average depth of the layers coincide well with the depth of the layers obtained by inversion of the local properties of the ground.

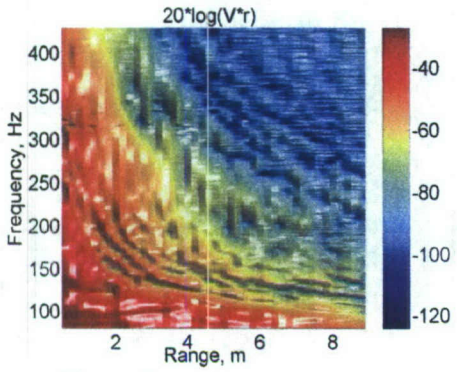

Figure 6

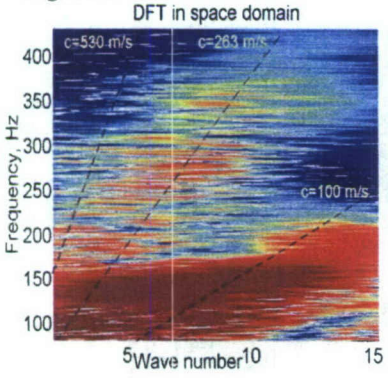

Figure 7

Estimation of local properties of the ground by the resonance technique

Along with average properties of the ground, the fluctuations of properties from point to point (or local properties) are very important for the creation of a model of false alarms. Consequently, a method for the determination of local properties of the ground was developed. Investigations of the acoustic-to-seismic transfer function (A/S *TF*) for a layered model of the ground show that positions of minima and maxima in the frequency dependent A/S *TF* have low sensitivity both to the parameters of the underlying substrate and the densities and attenuations in the upper layers. This fact permits the use of the resonance characteristics of the A/S *TF* for obtaining the ground properties. Two different techniques were developed and tested on the model and experimental data. The first technique is based on utilizing the angular dependence of the A/S *TF*. Estimation of only two parameters, namely C and D, are illustrated here. The best result may be obtained when the resonance frequency, the resonance amplitude, and the resonance half-width are used simultaneously for obtaining properties of the layered ground. The Figure 8 illustrates the results of estimating the ground properties (C – the sound speed and D – the layer thickness) from the synthesized numerical

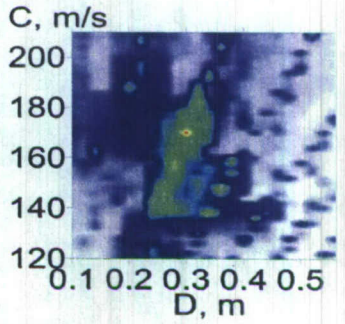

Figure 8.

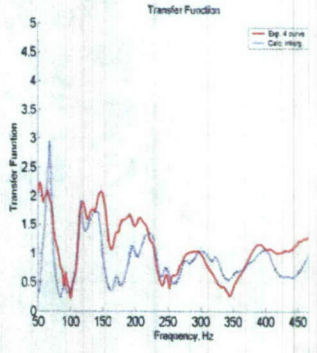

Figure 9.

data. The weighted function has a sharp global maximum (red spot, Figure 8) which permits determination the properties of the ground. Other parameters of the ground also may be determined.

A second technique was used to obtain local properties of the layered ground from outdoor measurements of the A/S *TF*. A combination of the resonance approach utilizing the frequency positions of the resonances along with the global search method was used for obtaining 17 parameters of the ground model which consisted of two elastic layers over an elastic substrate. In Figure 9, the measured frequency dependence of the TF is shown as a red curve. The blue curve in Figure 9 shows the results of reconstruction. It is easy to see that the basic features and even details (especially the small peaks in the vicinity of 90 Hz and 250 Hz) in the experimental and the numerical model data are in good agreement.

A model of false alarms

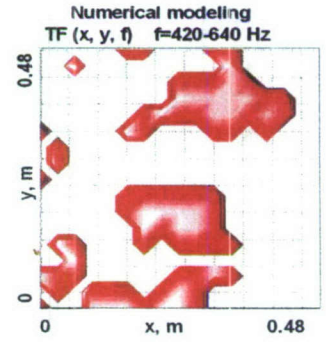

Figure 10

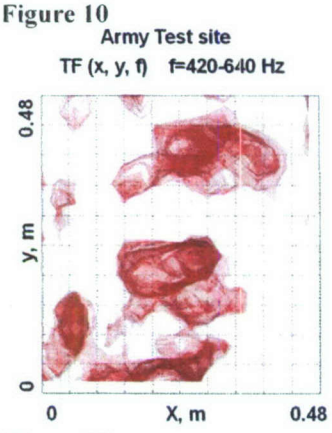

Figure 11

During the first year of investigation, the correlation between the positions of the wet spots on the ground and the positions of the high values of the A/S *TF* was revealed. A layered, visco-elastic model of the ground explaining this correlation was suggested. Further investigations confirm the validity of the suggested model. This model was used for numerical modeling of the spatial distribution of the high values of the A/S *TF*. During this modeling, it was speculated that the model of the ground with the wet spots consisted of two different elastic layers, covering the elastic substrate. The upper layer was less dense and had a lower sound speed than the second layer. The model of the ground outside of the wet spots consists of one elastic layer in which the parameters are equal to the parameters of the second layer in the wet spot model. The spatial distribution of the different models was estimated from the spatial distribution of the measured A/S *TF*. The result of the computation of the A/S *TF* is presented on the Figure 10. Strong correlation between the calculated (Figure 10) and measured (Figure 11) transfer functions is clearly seen. Thus, the suggested viscoelastic layered model may explain the nature of the strong response of the A/S *TF* and may be successfully used for calculations.

Spatial variability of the transfer function

Understanding of spatial variability of the TF is necessary for successful prediction of the probability of landmine detection in real environments. A laser Doppler vibrometer (LDV) was used for measurements of the A/S *TF*. During the LDV measurements, additional noise may be added to the A/S *TF*. The sound field interacting with the LDV excites vibrations in the LDV. These vibrations are added to the measured vibrations of the ground and may mask the frequency and spatial dependences of the A/S *TF*. The LDV vibrations have the same Fourier spectrum at all spatial points and can be eliminated by a simple processing of

$$TF_e(x,y,f) = TF(x,y,f) - \sum_x \sum_y TF(x,y,f). \quad (1)$$

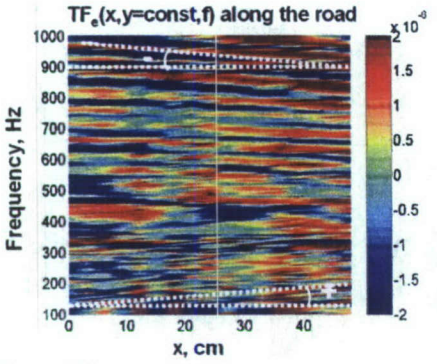

Figure 12

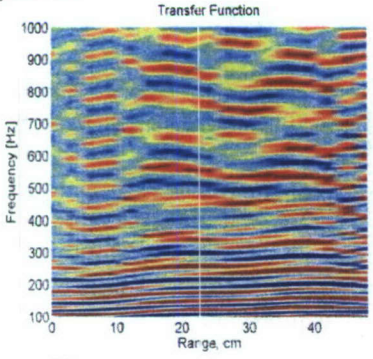

Figure 13

This operation makes spatial variations of the *TF* more visible. The spatial dependence of the $TF_e(x,y=const,f)$ (the section of the *TF* along the road) is shown in Figure 12. In Figure 12, one can see two sets of the color lines. The close lines with the positive angle with respect to the *x*-axis (+) are observed at the lower frequencies. The lines with the negative angle with respect to the *x*-axis (-) are observed at the higher frequencies. The spatial dependence of the $TF_e(x=const,y,f)$ (the section of the *TF* across the road) also has two sets of the lines, but both with positive inclinations. A model of the ground that incorporates the velocity variability data is necessary for explanation of this effect. Investigations of the A/S *TF* show that the frequency modulation in the A/S *TF* depends on the sound speed and the thickness of the layers. It is thought that the regular variability of the ground parameters combine with the random fluctuations of the parameters. The regular changes of the properties of the layers will lead to inclination of the lines of the local minima and maxima in the *TF*. Fluctuation of the parameters will lead to irregularities in this structure. It was also thought that different dependencies of the *TF* along and across the road were connected with the additional stress produced by the wheels of vehicles driving through the same place repeatedly. The model of the ground consisting of three elastic layers with the varying sound speed covering the elastic substrate was used to model the experimentally observed A/S *TF*. The results of the modeling of the A/S TF are shown on the Figure 13. One can see good qualitative agreement between calculated and measured TF. Therefore, it was shown that spatial fluctuation of the A/S TF may be successfully qualitatively modeled in the frame of the layered model of the ground which incorporates velocity variability data. Direct measurements of the compressional and shear velocities made on the dirt lane at the Army test site confirm existence of the different velocities in the areas of the lanes consistently driven over and areas that are less disturbed.

Summary of Soil Property Variations

A full discussion of these studies can be found at Reference [4], "Effect of variability of soil physical properties on clutter and false alarms in landmine detection," Reference [5], "Effect of ground variability on acoustic-to-seismic transfer function and false alarms in landmine detection," Reference [6], "Effect of ground variability on clutter and false alarms in landmine detection," Reference [7], "Determination of soil background parameters via acoustic-to-seismic transfer function," and Reference [8], "Influence of wheeled vehicular traffic on the acoustic-to-seismic transfer function."

Modeling

Substantial gains were made in the modeling of the phenomena underlying the acoustic mine detection technology. These gains are documented in Reference [9], "An effective fluid model for landmine detection using acoustic-to-seismic coupling" by Velea, Waxler, and Sabatier. Work was conducted on a finite-difference time-domain study of the effects of soil reconsolidation and is documented in Appendix A, "The effect of soil reconsolidation on acoustic mine detection."

Mine/Soil Models

NCPA also conducted studies for the development of an acoustic modal model of a mine/soil system to better understand the mine response. This effort resulted in a doctoral dissertation by W. C. Kirkpatrick Alberts II and is presented in Reference [10], "Resonance frequency shift saturation in acoustic landmine detection experiments," and Reference [11], "Studying the mechanical behavior of a plastic, shock-resisting, anti-tank landmine."

Many, if not all, of the plastic landmines contain detonating mechanisms that are shock resistant. These mechanisms result in the top plate of the mine being acoustically compliant, or soft, compared to the soil and it is this contrast property that makes these mine types easy to detect. Acoustic models of these mines have been based on the simple harmonic oscillator (SHO) which results in the classical magnitude and phase resonance responses. At the resonance, the velocity magnitude goes through a maximum and the phase goes through zero. For most mines, the 'Q' of the resonances are not large and the magnitude and phase effects are often weak. There have been several papers describing how the frequency of the resonance will change with added mass. Donskoy has proposed SHO models that included shear effects as well as the added mass or soil acting as a thin plate. Others, including Korman and Sabatier, and as well Donskoy, have conducted laboratory experiments in which mass was added to the top plate of mines and even mine surrogates. As the mass, representing soil, is increased in these model experiments, various results for changes in the resonant frequency have been reported. Most prevalent is data suggesting that the resonant frequency first decreases and then dramatically increases with added mass.

Figure 14 shows resonance frequency as a function of mine depth and comparison with predictions of Donskoy's coupled oscillators model (D. Donskoy, A. Ekimov, N. Sedunov, and M. Tsionskiy, "Nonlinear seismo-acoustic land mine detection and discrimination," J. Acoust. Soc. Am., 111(6), 2705-2714 (2002)) and Velea's effective fluid model, (D. Velea, R. Waxler, and J. M. Sabatier, "An effective fluid model for landmine detection using acoustic to seismic coupling," J. Acoust. Soc. Am., 115 (5), 1993-2002 (2004)). Donskoy's lumped element or coupled harmonic oscillator model predicts a continuous reduction in the resonant frequency as mass is added to the landmine, the addition of soil shear strength reduces the rate at which the frequency decreases, while Velea's effective fluid model predicts a saturation of the resonant frequency with increasing depth. Donskoy published the two coupled oscillators, without shear and later added soil shear and then Zagrai published the soil plate SHO model (A. Zagrai, D. Donskoy, and A. Ekimov, "Structural vibrations of buried land mines," J. Acoust. Soc. Am., 118 (6), 3619-3628 (2005)). The solid line in Figure 16 shows Zagrai's SHO model with the soil acting as a plate and shows that the resonant frequency first decreases and then increases monotonically as mass is added to the landmine.

In Figure 15, the magnitude of the ground surface particle velocity response for a point or pixel directly over a VS2.2 plastic antitank landmine buried at six different depths in a weathered gravel lane is shown. For this field data there is no clear trend for the frequency of the resonance to either decrease or increase. However, if one neglects the results for the 1 or the 2 inch depth, there is a trend for the resonant frequency to first decrease and then slightly increase.

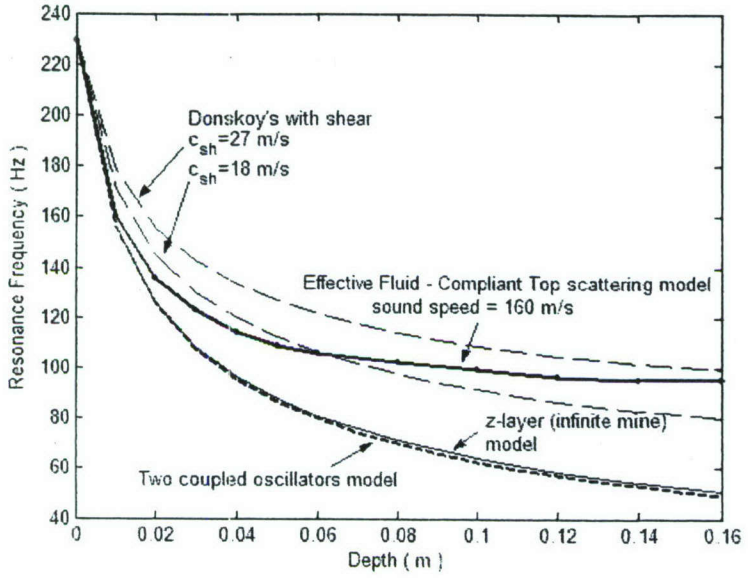

Figure 14. Resonance frequency as a function of mine depth: comparison between the predictions of Donskoy's coupled oscillators model and Velea's effective fluid model.

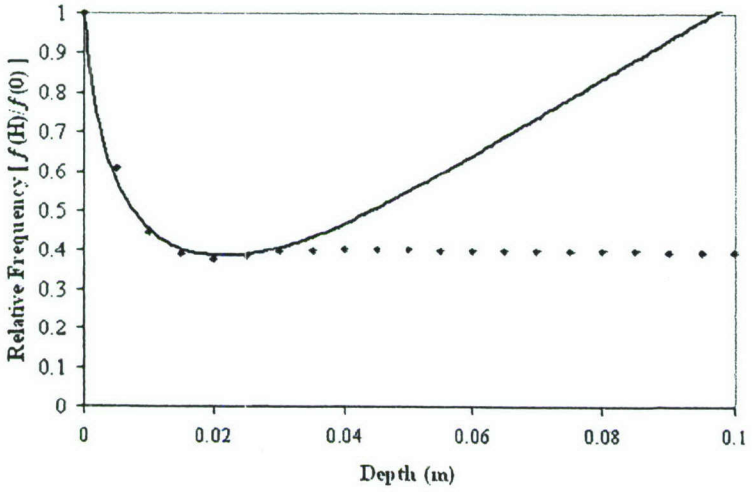

Figure 15. This chart shows the resonance frequency shift versus burial depth of the first symmetric mode of a mine simulant (solid squares) and a theoretical curve (solid line) produced from Zagrai's coupled plate model

Signal Processing

NCPA performed research in signal processing by investigating alternative methods for signal processing. These included new techniques for analysis and for image processing.

Wavelet Analysis

A time-scale, linear method (wavelet analysis) was utilized for improving the probability of landmine detection. It has been shown that the wavelet map of the frequency dependence of the normal particle velocity at different spatial points provides additional information about the

structure of the acoustic-to-seismic transfer function. Wavelet analysis of the measured signals resulted in typically stable characteristics for the undisturbed ground, the disturbed ground, and the ground with a mine. These characteristics may be used for the discrimination of false alarms and as an additional criterion to find mines that are hard to locate by traditional methods. A further description of this research may be found in Reference [12], "Wavelet analysis for landmine detection false alarm discrimination."

Image Processing

A new image processing technique based on phase information was developed and employed to assist in rejecting false alarms. The phases of the ground's surface particle velocity for both off-target and on-target locations offer contrast to aid in the detection of mines. In raw, unprocessed images of the magnitude and phase of the ground's surface particle velocity as a function of frequency, the strongest contrast image for the magnitude appears at a lower frequency than for the phase contrast image. Simple harmonic oscillator models of the soil/mine system suggest that one look for the zero crossing in the phase response for pixels over the mine as a detection criterion. However, both particle velocities measured in field tests and plane wave, elastic layered models of the ground's phase response show many phase zero crossings for off-target or background locations, thus precluding zero crossings as a stand alone indicator for the presence of a mine. Also both these models and field measurements show that the complex velocity response of the ground becomes spatially more random as the frequency increases. For frequencies above the mine resonance, both coupled oscillator and plane wave acoustic models show the phase of the soil particle velocity becomes constant between the first resonance and first anti-resonance of the soil/mine system. This is observed in many scans of field data as indicated in the images shown in Figure 16. This figure shows magnitude and phase from 90 to 340 Hz in 20Hz-wide bands. With increasing frequency, the magnitude image is clear before the phase image and is fading much faster than the phase image. For space reasons, the data below 90 Hz and above 340 Hz is not shown, but the magnitude image is present at lower frequencies than shown in this figure and the phase image is clear above frequencies reported here.

Earlier work on image processing to detect mines from the ground's particle velocity magnitude data used three image processing criteria. These were contrast ratio for the velocity magnitude on and off the target, the spatial size of the contrast region and the persistence of the contrast over a frequency band of at least 40 Hz. We have developed phase criteria that are being used in image processing algorithms. These criteria are that both the magnitude and phase signatures span a contiguous frequency band of at least 40 Hz. The frequency centroid of the magnitude signature lies below the frequency centroid of phase signature. And, both signatures spatially overlap, i.e. the Euclidean distance between the two spatial centroids is less than three pixels when the pixel size is 7cm. This is being tested for antitank mines at this time. Thus far and over the next year we are developing image processing algorithms to take advantage of the phase response of the ground for mine detection with the specific goal of improving P_d and reducing P_{FA}. This is discussed more fully in Reference [13], "Apparatus and algorithms for acoustic landmine detection."

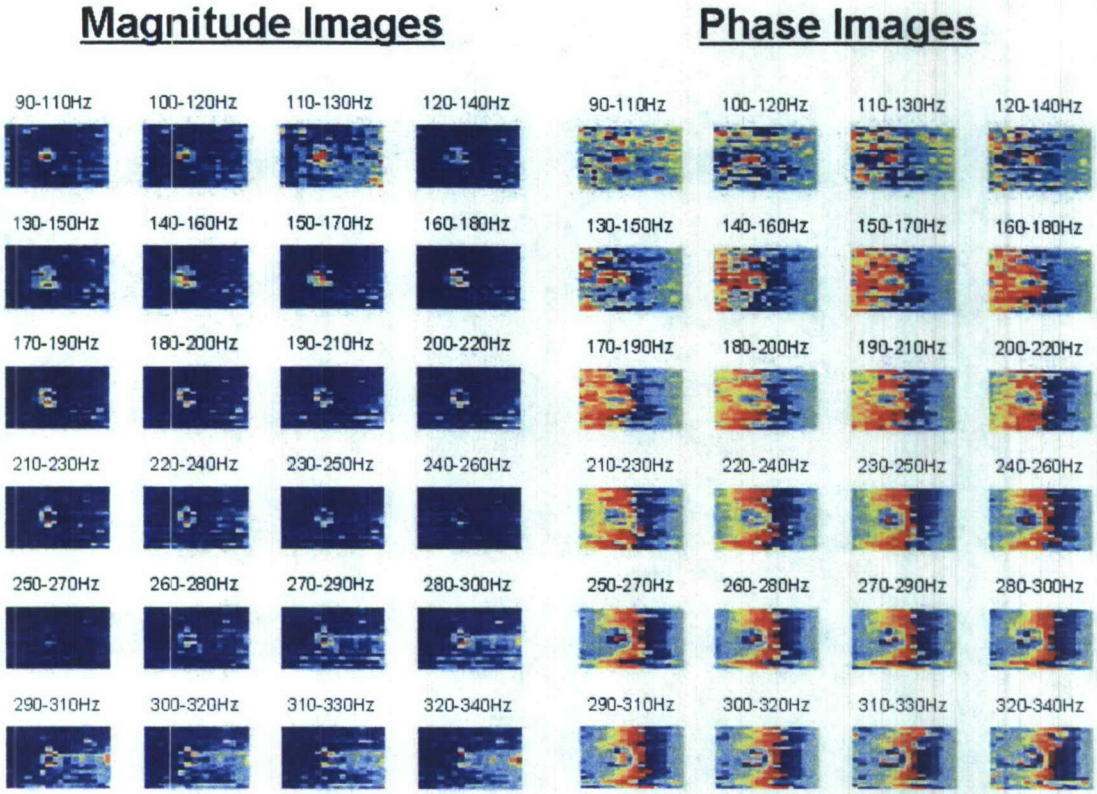

Figure 16. Magnitude and phase velocity images of a EM12 antitank landmine simulant.

5.0 BIBLIOGRAPHY

- Publications in Peer-Reviewed Journals
  - V. N. Fokin, M. S. Fokina, J. M. Sabatier, N. Xiang, and W. B Howard, "Effect of variability of soil physical properties on clutter and false alarms in landmine detection," Radio Sci., 39, RS4S04 (2004)
  - Vladimir N. Fokin, Margarita S. Fokina, James M. Sabatier, and Zhiqu Lu, "Effect of ground variability on acoustic-to-seismic transfer function and false alarms in landmine detection," J. Acoust. Soc. Am., 120(2), 621-630 (2006).
  - D. Velea, R. Waxler, and J. M. Sabatier, "An effective fluid model for landmine detection using acoustic to seismic coupling," J. Acoust. Soc. Am., 115 (5), 1993-2002 (2004).
  - W. C. Kirkpatrick Alberts II, James M Sabatier, Roger Waxler, "Resonance frequency shift saturation in acoustic landmine detection experiments," J. Acoust. Soc. Am. 120(4), 1881-1886 (2006)
  - W. C. Kirkpatrick Alberts II, Roger Waxler, and James M Sabatier, "Studying the mechanical behavior of a plastic, shock-resisting, anti-tank landmine," J. Acoust. Soc. Am. 120(6), 3655-3663 (2006).
- Publications in Conference Proceedings

- Margarita S. Fokina, Vladimir N. Fokin, and James M. Sabatier, "Effect of ground variability on clutter and false alarms in landmine detection," Proc. SPIE, Vol. 5415, 156-166 (2004)
- Vladimir N. Fokin, Margarita S. Fokina, and James M. Sabatier, "Determination of soil background parameters via acoustic-to-seismic transfer function," Proc. SPIE, Vol. 5415, 30-34 (2004)
- Vladimir N. Fokin, Margarita S. Fokina, James M. Sabatier, "Wavelet analysis for landmine detection false alarm discrimination," Proc. SPIE, Vol. 5794, 601-611 (2005)
- Margarita S. Fokina, Vladimir N. Fokin, Zhiqu Lu, and James M. Sabatier, "Influence of wheeled vehicular traffic on the acoustic-to-seismic transfer function," Proc. SPIE, Vol. 5794, 577-589 (2005).
- Ghaith M. Matalkah; Mustafa M. Matalgah; James M. Sabatier, "CFAR detection algorithm for acoustic-seismic landmine detection," Proc. SPIE, Vol. 6553, DOI: 10.1117/12.719754 (2007).

- Presentations at Professional Meetings
  - Vladimir M. Fokin, Margarita S. Fokina, James M. Sabatier, and Wheeler B. Howard, "Geoacoustic inversion via acoustic-seismic transfer function", J. Acoust. Soc. Am., 114 2457 (2003).
  - Margarita Fokina, Vladimir Fokin, James M. Sabatier, and Ning Xiang, "Effect of ground variability on the acoustic-seismic transfer function", J. Acoust. Soc. Am., 114 2457 (2003).
  - Margarita S. Fokina and James M. Sabatier, "Acoustic-to-seismic transfer function attribute for discrimination of false alarms and landmine detection," J. Acoust. Soc. Am., 116 2494 (2004).
  - Vladimir N. Fokin, James M. Sabatier, and Wheeler B. Howard, "Modal analysis of broadband acoustic signals propagating in the top layer of the ground," J. Acoust. Soc. Am. 116, 2494 (2004).
  - Vladimir N. Fokin, Margarita S. Fokina, and James M. Sabatier, "False alarms associated with the acoustic-to-seismic detection of buried landmines," J. Acoust. Soc. Am. 115, 2417 (2004).
  - Margarita S. Fokina, Vladimir N. Fokin, and James M. Sabatier, "Effects of elasticity and porosity in modeling of the acoustic-to-seismic transfer function," J. Acoust. Soc. Am. 115, 2384 (2004).
  - Chris McNeill and James Sabatier, "Angle of Incidence Seismic/Acoustic Ratios," Mid-South Area Engineering and Sciences Conference, University, MS 17-18 May 2007.
  - Robert Lirette, Thomas Muir and James Sabatier, "Acoustic Saturation of Plane and Spherical Waves in Air, Mid-South Area Engineering and Sciences Conference, University, MS 17-18 May 2007.

8.0 GRADUATE STUDENTS SUPPORTED

- Doctoral dissertation completed: W. C. K. Alberts II, "A study of the acoustic behavior of a plastic blast hardened antitank landmine," University of Mississippi, October 2005.
- Master's thesis completed: G. Matalkah, "Apparatus and algorithms for acoustic landmine detection," University of Mississippi, May 2007.
- Christopher A. McNeill, Master of Science candidate, Physics
- Robert Lirette, Master of Science candidate, Physics

- Gregory Broussard, Doctor of Philosophy candidate, Physics

9.0 REFERENCES

[1] J. M. Sabatier, "Acoustic Technology for Landmine Detection", Final Report, Contract Number: DAAB07-97-C-6040, NCPA Report JS0700-01, 2001, 66 pages.

[2] J. M. Sabatier, "Acoustic Technology for Landmine Detection", Final Report, Contract Number: DAAB15-00-C-1005, NCPA Report JS0303-01, 2003, 387 pages.

[3] J. M. Sabatier, "Fusion of Acoustic and Ground Penetrating Radar Sensors," Final Report, Contract Number: DAAB15-02-C-0024, NCPA Report JS0807-01, 82 pages.

[4] V. N. Fokin, M. S. Fokina, J. M. Sabatier, N. Xiang, and W. B Howard, "Effect of variability of soil physical properties on clutter and false alarms in landmine detection," Radio Sci., **39**, RS4S04 (2004).

[5] Vladimir N. Fokin, Margarita S. Fokina, James M. Sabatier, and Zhiqu Lu, "Effect of ground variability on acoustic-to-seismic transfer function and false alarms in landmine detection," J. Acoust. Soc. Am., **120**(2), 621-630 (2006).

[6] Margarita S. Fokina, Vladimir N. Fokin, and James M. Sabatier, "Effect of ground variability on clutter and false alarms in landmine detection," Proc. SPIE, Vol. 5415, 156-166 (2004).

[7] Vladimir N. Fokin, Margarita S. Fokina, and James M. Sabatier, "Determination of soil background parameters via acoustic-to-seismic transfer function," Proc. SPIE, Vol. 5415, 30-34 (2004).

[8] Margarita S. Fokina, Vladimir N. Fokin, Zhiqu Lu, and James M. Sabatier, "Influence of wheeled vehicular traffic on the acoustic-to-seismic transfer function," Proc. SPIE, Vol. **5794**, 577-589 (2005)

[9] Doru Velea, Roger Waxler, and James M. Sabatier, "An effective fluid model for landmine detection using acoustic to seismic coupling", J. Acoust. Soc. Am., **115** (5), 1993-2002 (2004).

[10] W. C. Kirkpatrick Alberts II, James M Sabatier, Roger Waxler, "Resonance frequency shift saturation in acoustic landmine detection experiments," J. Acoust. Soc. Am. **120**(4), 1881-1886 (2006)

[11] W. C. Kirkpatrick Alberts II, Roger Waxler, and James M Sabatier, "Studying the mechanical behavior of a plastic, shock-resisting, anti-tank landmine," J. Acoust. Soc. Am. **120**(6), 3655-3663 (2006).

[12] Vladimir N. Fokin, Margarita S. Fokina, James M. Sabatier, "Wavelet analysis for landmine detection false alarm discrimination," Proc. SPIE, Vol. 5794, 601-611 (2005).

[13] G. Matalkah, "Apparatus and algorithms for acoustic landmine detection," Master of Science Thesis, University of Mississippi, May 2007.

Appendix A

The effect of soil reconsolidation on acoustic mine detection

L. Dwynn Lafleur

*National Center for Physical Acoustics, The University of Mississippi, University, Mississippi 38677**

(Dated: 13 August 2004)

This report describes a finite-difference time-domain study of the effects of soil reconsolidation on the detection of buried mines using acoustic-seismic coupling. The ground is modeled as a semi-infinite elastic solid containing a surface layer of lower density and elastic moduli. The mine, modeled as a soft elastic slab, is buried within the surface layer of the ground. It is insonified by a loudspeaker in the air to one side of the mine. The calculations show that when the soil above the mine has low density and elastic moduli characteristic of unconsolidated soil, a large difference exists between the on-target and off-target seismic response of the ground surface near the mine. However, when the soil becomes reconsolidated, the seismic contrast is greatly diminished. This agrees with observations in the field.

I. INTRODUCTION

When a land mine is deployed, the usual procedure is to dig a shallow hole in the soil, place the mine at the bottom of the hole, then refill the hole with the excavated soil. This process necessarily leaves the soil above the mine in a relatively unconsolidated state. Over the period of several months or years, depending on local weather, the soil over the mine gradually reconsolidates and approaches the form of the undisturbed soil surrounding the mine.

Over the past few years, the National Center for Physical Acoustics has shown the feasibility of using acoustic-seismic coupling to detect buried land mines. The technique employs a loudspeaker to generate sound waves in air and a laser doppler vibrometer (LDV) to detect a difference between the resulting vibration amplitude of the ground surface above the center of the mine (on-target) and the surface away from the mine (off-target). Measurements have been performed at Fort A. P. Hill on mines both soon after burial and several years after burial. The earlier measurements show a large difference between the on-target and off-target signals, but that difference is significantly diminished in the later measurements.

This report describes a finite-difference time-domain (FDTD) study of this effect. The calculations are limited to wave disturbance in two dimensions (*P-SV* waves) and thus cannot be expected to be *quantitatively* accurate. Instead, the work is an attempt to verify the effect of reconsolidation *qualitatively* in hopes of leading to a better understanding of the physics involved and perhaps aid in offsetting the negative consequences of the effect.

II. NUMERICAL PROCEDURE

A. The FDTD method

The finite-difference method described in this report is based on earlier work by Virieux[1] and Collino and Tsogka[2]. The latter study who used the same FDTD method as the first but with a more recent and superior absorbing boundary condition, the perfectly matched layer.[3]

The method involves a time-domain calculation in two spatial dimensions; thus, wave variables are assumed uniform in the third dimension. The medium in the calculation method may be

heterogeneous, but it is assumed to be *locally* isotropic so that only two elastic constants, e.g., the Lamé constants λ and μ, are needed to specify its elastic properties at each position. In addition, the spatial dependence of the density must be provided.

Wave propagation is formulated in terms of the two components of particle velocity, the two components of normal stress, and the single shear stress component as appropriate for *P-SV* waves in two-dimensions. The method is based on the constitutive relations and first-order differential equations of motion relating the particle velocity and stress. Use of a staggered grid gives a procedure with second-order accuracy. For further details, see Refs. 1 and 2.

Computations based on the above method are performed on a personal computer using a combination of a *Mathematica* notebook and a compiled program consisting of Fortran subroutines with a C front-end interface. The user enters the numerical parameters of the FDTD simulation and the functions describing the medium, source, and receivers in the *Mathematica* environment, where *Mathematica*'s calculation and graphics abilities aid in determining input values and functions. These data are then passed to the compiled Fortran subroutines via *Mathematica*'s *MathLink* feature, which connects with the C interface in the compiled program. The Fortran subroutines perform the actual time stepping of the FDTD method, writing the results to files. (The use of compiled Fortran for the time stepping greatly reduces the calculation time from that required were the calculations performed in the interpretive *Mathematica* environment.) The *Mathematica* notebook then reads the files and performs the numerical and graphic analysis of the results as desired by the user.

B. Medium properties

The study reported here models wave propagation in a heterogeneous medium consisting of a semi-infinite fluid (i.e., air) above a semi-infinite elastic solid (i.e., ground). The ground is assumed to consist of a 0.30-m-thick surface layer of relatively low elastic moduli atop a semi-infinite solid of higher elastic moduli, an approximation to the top two meters of ground at the "gray gravel lane" at Fort A. P. hill.[4] Since an FDTD calculation is limited to a grid of finite extent, the medium in the calculation was 2.00 m wide and 2.00 m tall, with its center at the surface of the ground directly above the center of the mine. (See below.)

The properties of the materials constituting the medium are shown in Table I, where ρ is the density and λ and μ are the Lamé parameters of the media. The quantities listed for "ground, ... " are based on seismic measurements[4] of the gray gravel lane at Fort A. P. Hill. Since no measurements were available for unconsolidated soil, values based on measured properties of pumice[5] were used.

TABLE I. Properties of portions of the heterogeneous medium in the FDTD study. Shown are the density ρ and Lamé parameters λ and μ.

Medium	ρ (kg/m^3)	λ (Pa)	μ (Pa)
air	1.21	1.42×10^5	0
ground, surface layer	1700	1.04×10^8	1.20×10^7
ground, lower region	1700	3.92×10^8	3.93×10^7
unconsolidated soil	660	3.00×10^6	1.06×10^6

C. Source properties

The loudspeaker used as a source in the acoustic mine detection technique was modeled as a 0.50-m-tall vertical plane containing a uniform distribution of monopole stress sources of identical strength and time dependence. The assumed time dependence was the time-differentiated Gaussian pulse

$$F(t) = A \cdot (t - 1/f_0) \exp\left[-4\pi f_0^2 (t - 1/f_0)^2\right], \tag{1}$$

where A is a scaling constant in units of pascals per second and f_0 is the (amplitude-weighted) average frequency of the signal. Since the FDTD method is based on linear theory, the results are independent of source amplitude except for scaling. In order to yield particle velocities convenient in scaling of graphs, $A = \rho_f c_{pf} f_0$ was used, where ρ_f and c_{pf} are the density and P-wave speed, respectively, in the surface layer of the ground. The average frequency for the calculations chosen was $f_0 = 200$ Hz. With these values, the source signal is as shown in Fig. 1.

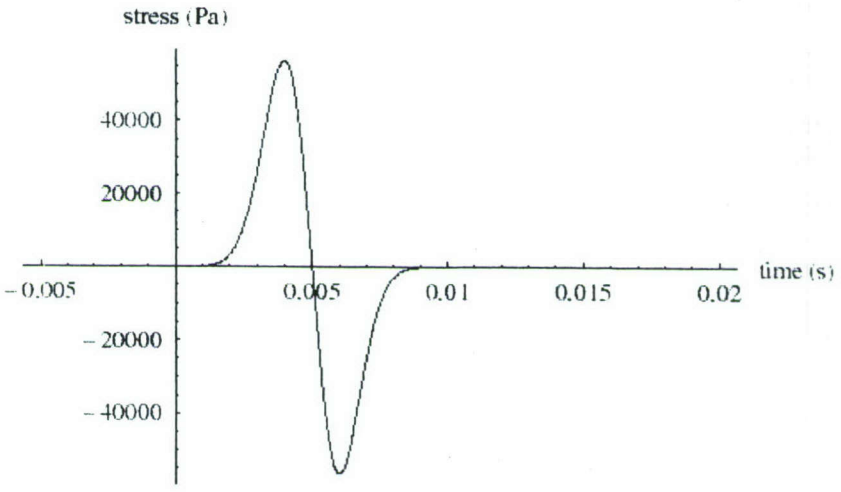

FIG. 1. Source signal used in this study.

In all calculations, the bottom edge of the source plane was located 0.10 m above the ground and at a horizontal distance of 1.00 m from the nearer edge of the mine.

D. Mine properties

Experimental modal analysis of the vibrations of the top plates of several mines in air have shown a minimum resonance frequency of about 260 Hz.[6] In the FDTD study reported here, the mine is modeled as a 0.30-m-wide, 0.10-m-thick slab of soft material of density 1000 kg/m^3 and Lamé parameters λ and μ of 4.64×10^6 Pa and 3.09×10^6 Pa, respectively. When resting on a rigid surface, such a slab has a quarter-wave thickness resonance frequency of 260 Hz.

In FDTD simulations with the mine present, the mine was always positioned with its major surfaces horizontal and its top 0.10 m below the ground surface. As mentioned above, the mine was always a horizontal distance of 1.00 m from the source.

E. Receiver (LDV measurement) locations

The FDTD program provides for the placement of an arbitrary number of point receivers in the medium. Each of these receivers records the time history all five wave disturbances (two components of particle velocity and three elements of stress) at its location. The only receiver signals presented in this report are vertical components of particle velocity at the ground surface; thus, the receivers are simulating LDV measurements.

The same linear array of five receivers was used in all calculation. The five points of measurements were all on the ground surface, with the central receiver (Receiver 3) of the array directly over the center of the mine. The outer two receivers (Receivers 1 and 5) were each 0.30 m from the center of the array, i.e., 0.15 m beyond the outer edge of the mine. The other two receivers (Receivers 2 and 4) were each 0.12 m from the center of the array, i.e., 0.03 m inside the outer edge of the mine.

F. Case studies

FDTD simulations were performed for three cases: (1) no mine present, (2) the mine present and occupying the bottom half of a 0.30-m-wide, 0.20-m deep hole, the top half filled with unconsolidated soil, and (3) the same as the previous case with the consolidated soil replaced by the original surface layer material, i.e., reconsolidated soil.

III. RESULTS

A. Case 1: No mine

Figure 2 shows the distributions of the horizontal component (U) and vertical component (V) of the particle velocity 5.00 ms after the source starts emitting the wave corresponding to the signal shown in Fig. 1. Since the acoustic impedance of the ground is so much greater than that of air, the wave penetration into the ground is invisible on the scale used in the figure. Note that the vertical component of velocity near the ground is very low. Since the average wavelength of the acoustic radiation in air is over 3 m and the ground is relatively rigid, the surface is almost a vertical velocity node.

If the color scale is reduced, the distribution of particle velocity in the sub-surface region is visible, as shown in Fig. 3. Here, we see the initial penetration of the *P*-wave through the surface layer and into the bottom region.

Figure 4 shows two later distributions of particle velocity. Inspection of the velocity distribution figures between the two shown here indicates that the local maximum in V near the surface at approximately $x = -0.4$ m in Fig. 4(a) is the same that near $x = 1.5$ m in Fig. 4(b). Thus, the maxima and minima near that peak are associated with either a true surface wave or a wave traveling inside the wave guide formed by the upper and lower boundaries of the surface layer.

The vertical components of the particle velocity recorded by the receivers are shown in Fig. 5. Given that Receiver 1 through Receiver 5 are progressively farther from the source, we see the expected later arrival of respective maxima and minima from one receiver to the next. However, the shapes of portions of the signals vary among the receivers, indicating interference effects.

The absolute values of the Fourier transforms of the signals in Fig. 5 are shown in Fig. 6, along with that of the source signal, Fig. 1. It is clear from these figures that the ground forms a band-

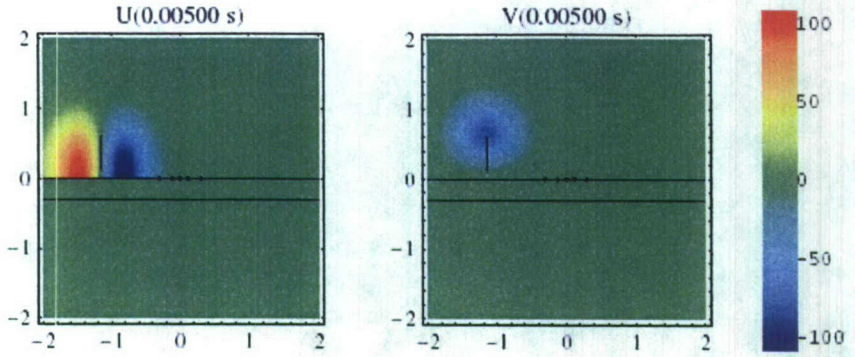

FIG. 2. Particle velocity distribution in the air at time t = 5 ms. U and V are the horizontal and vertical components, respectively. Note the location of the ground surface at $z = 0$, the bottom of the surface layer at $z = -0.30$ m, and the linear array of five receivers at the ground surface.

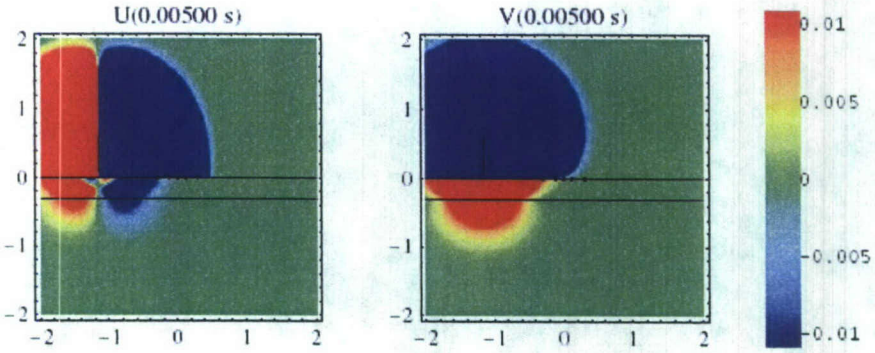

FIG. 3. Particle velocity distribution in the ground at time t = 5 ms with no mine present. Note the color scale is reduced from that in Fig. 2

pass filter for the vertical velocity components detected by the receivers. Fourier amplitudes in the frequency band from approximately 120 Hz to approximately 220 Hz are attenuated in the receiver signals at all locations.

B. Case 2: Mine beneath unconsolidated soil

The particle velocity distribution at t = 45 ms with the mine beneath unconsolidated soil is shown in Fig. 7. Here we see that reflections from discontinuities in the surface layer due to the hole produce much different velocity distributions in the layer than that in Fig. 4 (b). In addition, the mine and unconsolidated soil cause waves to be broadcast back into the air more efficiently than in the previous case.

Figure 8 shows the receiver signals for this case. Comparing with Fig. 5, we see that the most obvious difference is the reduction of the signals detected by the outer receivers.

The absolute value of the Fourier transforms of the signals in Fig. 8 are shown in Fig. 9. As expected from the signals, we see a dramatic reduction in response of the off-target receivers at all frequencies. The on-target receiver shows a significantly stronger signal a virtually all frequencies.

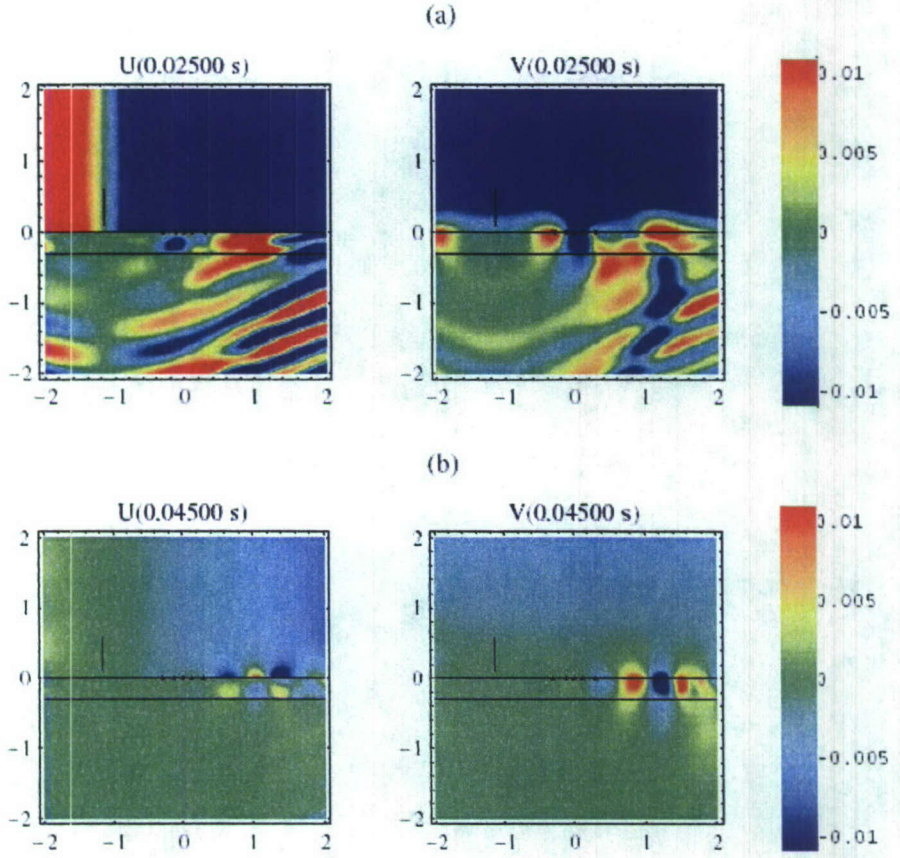

FIG. 4. Particle velocity distribution in the ground at times (a) t = 25 ms and (b) t = 45 ms with no mine present.

suggesting easy detection by the acoustic-seismic method.

C. Case 3: Mine beneath reconsolidated soil

The receiver signals for the mine beneath reconsolidated soil, i.e., the same medium as the rest of the surface layer, are shown in Fig. 10. Comparing these signals to those in Fig. 8, we see that the strength of the off-target signals has returned. In addition, the signals in this case are stronger that those recorded in the absence of the mine (Fig. 5).

Figure 11 shows the absolute value of the Fourier transforms of the receiver signals with the mine beneath reconsolidated soil. When these results are compared with Fig. 6, it is seen that the band-pass filter effect is no longer present, explaining the difference in the signals with and without the mine as noted above.

However, in comparing Fig. 11 with Fig. 9, we see that the large contrast between the on-target and off-target signals seen with unconsolidated soil no longer exists. This is the unfortunate result observed in actual field measurements as mentioned in the Introduction.

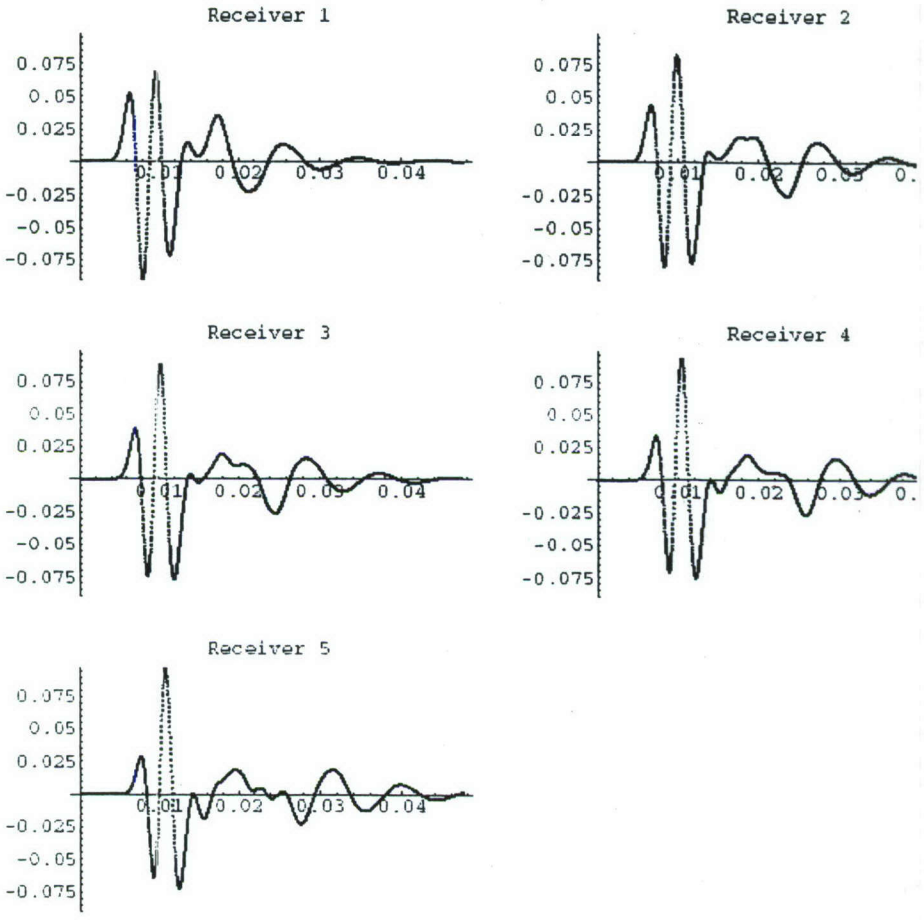

FIG. 5. Vertical components of the particle velocity at the five receiver locations with no mine present. The coordinates of the receivers are given in the text. Receivers 1 and 5 are the outermost and Receiver 3 is over the center of the mine.

IV. CONCLUSION

This report has described an FDTD study of the effect of soil reconsolidation on the sensitivity of acoustic mine detection. Preliminary analysis has shown that, in agreement with experimental measurements, a loss in on-target-to-off-target contrast occurs when the soil above a mine is reconsolidated.

Further analysis of the detailed output of the FDTD simulation is being performed. It is hoped that several features demonstrated by the study will be better understood, especially the interesting phenomena related to wave propagation along the surface layer. Realizing the physics involved in these phenomena is an important part of understanding the process of acoustic mine detection.

---

* Electronic address: lafleur@louisiana.edu; Permanent address: Department of Physics, University of Louisiana at Lafayette, Lafayette, Louisiana 70504

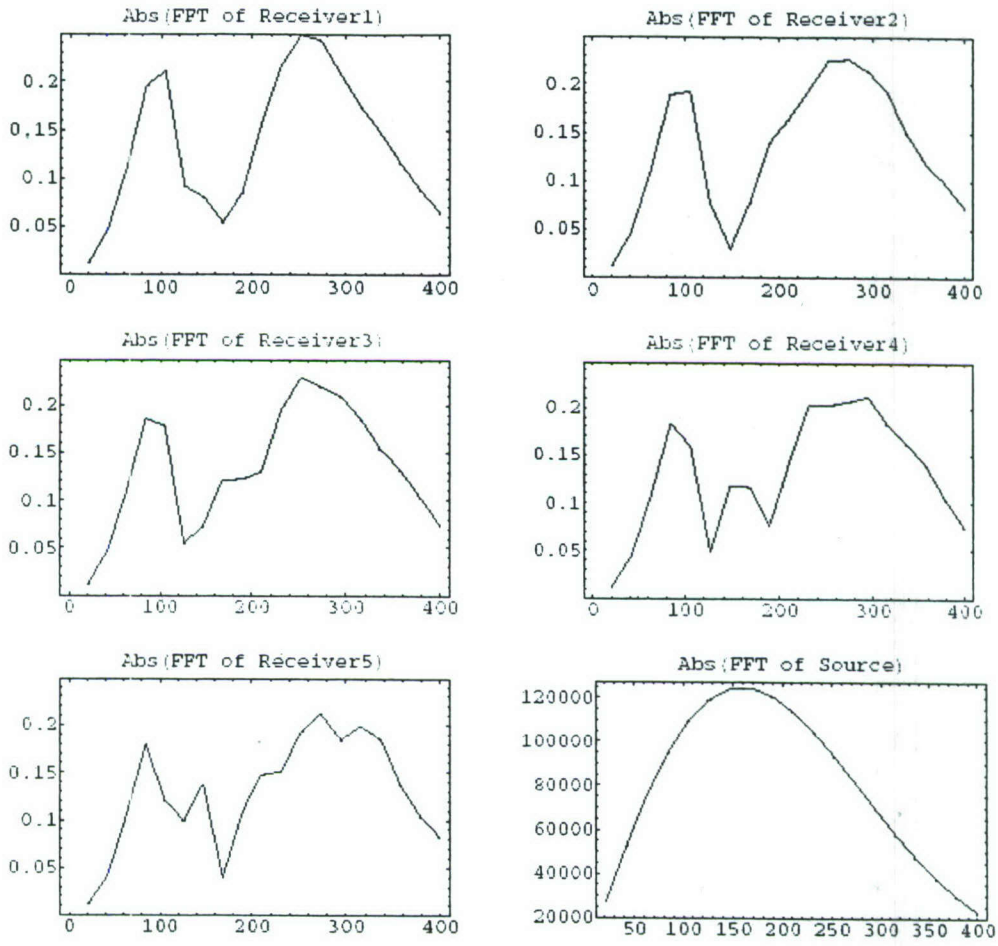

FIG. 6. Absolute values of the Fourier transforms of the receiver signals with no mine present, along with that of the source signal.

[1] J. Virieux, "*P-SV* wave propagation in heterogeneous media: Velocity-stress finite-difference method," Geophysics **51,** 889–901 (1986).

[2] F. Collino and C. Tsogka, "Application of the perfectly matched absorbing layer model to the linear elastodynamic problem in anisotropic heterogeneous media," Geophysics **66,** 294–307 (2001).

[3] J.-P. Bérenger, "A Perfectly Matched Layer for the Absorption of Electromagnetic Waves," J. Comput. Phys. **114,** 185–200 (1994).

[4] J. L. Llopis, private communication (unpublished).

[5] J. M. Sabatier, H. E. Bass, and G. R. Elliott, "On the location of frquencies of maximum acoustic-to-seismic coupling," J. Acoust. Soc. Am. **80,** 1200–1202 (1986).

[6] W. C. K. Alberts, private communication (unpublished).

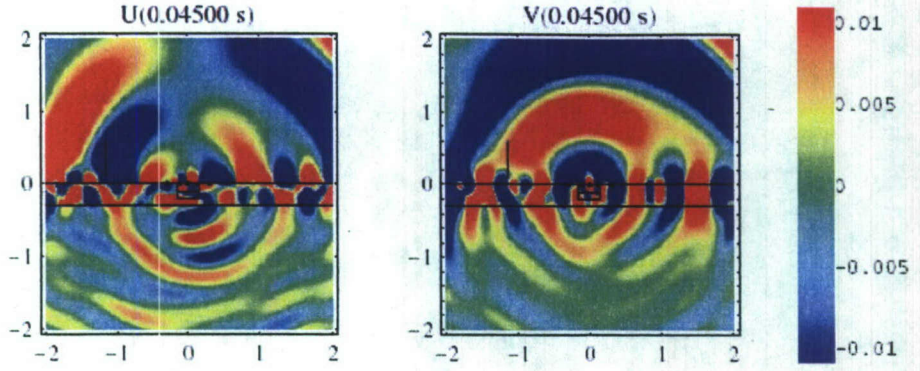

FIG. 7. Particle velocity distribution in the ground at time t = 45 ms in the presence of a mine beneath unconsolidated soil. Compare to Fig. 4 (b).

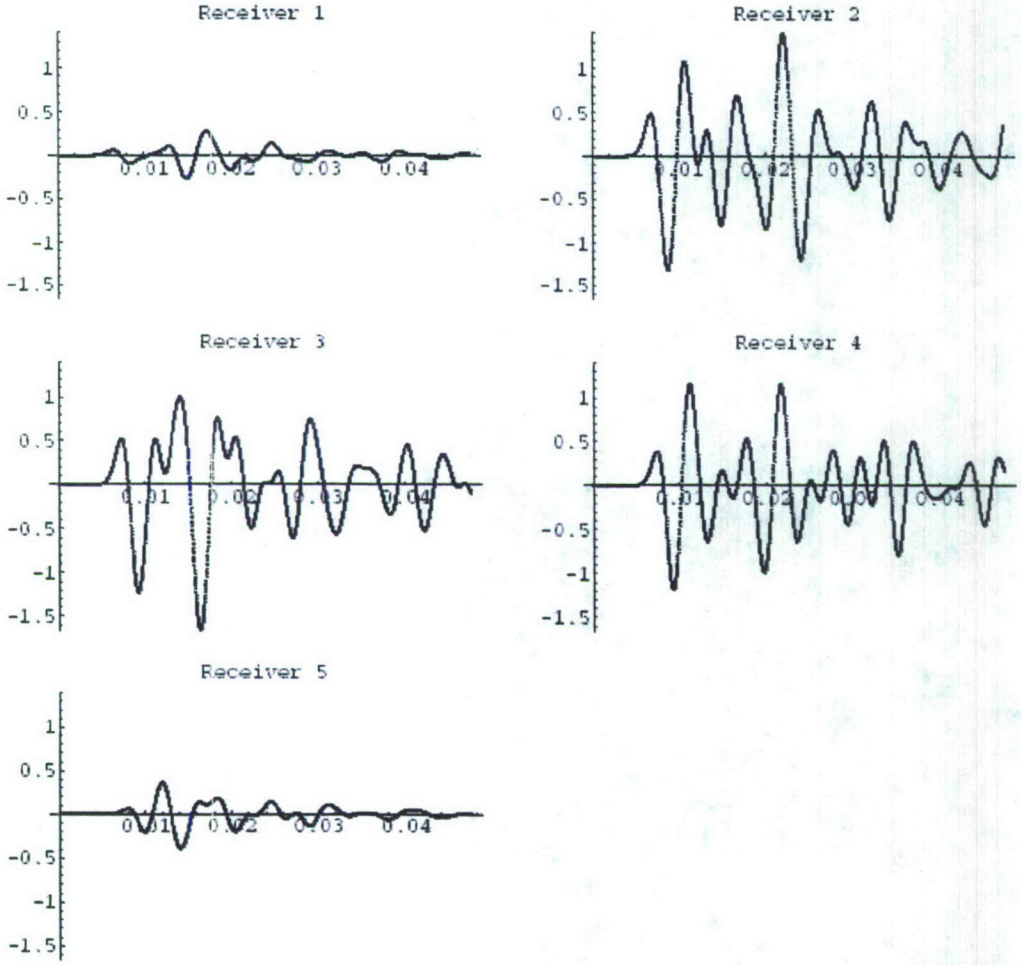

FIG. 8. Vertical components of the particle velocity at the five receiver locations with a mine beneath unconsolidated soil. Recall that Receivers 1 and 5 are the outermost and Receiver 3 is over the center of the mine.

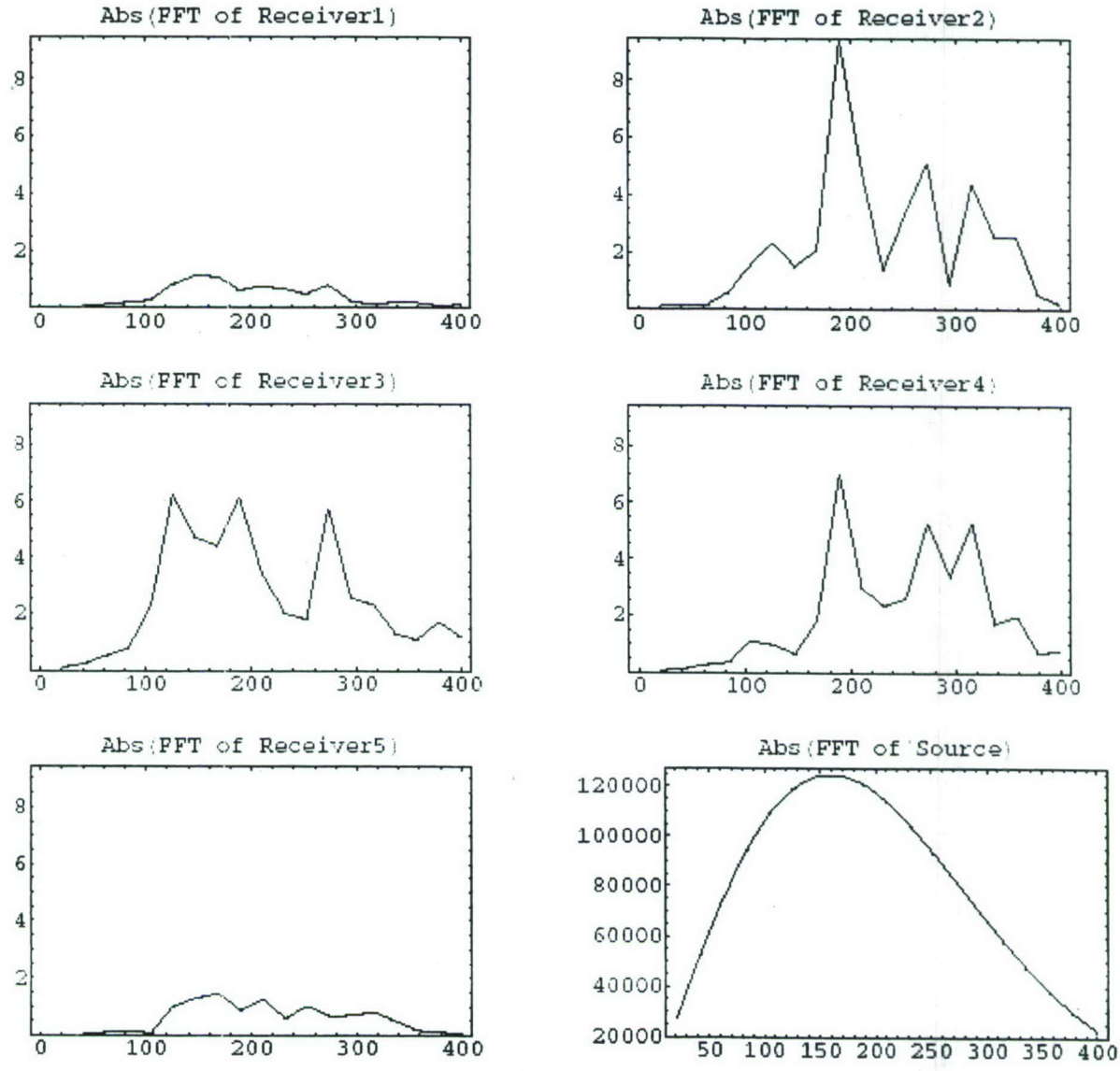

FIG. 9. Absolute values of the Fourier transforms of the receiver signals with a mine beneath unconsolidated soil, along with that of the source signal

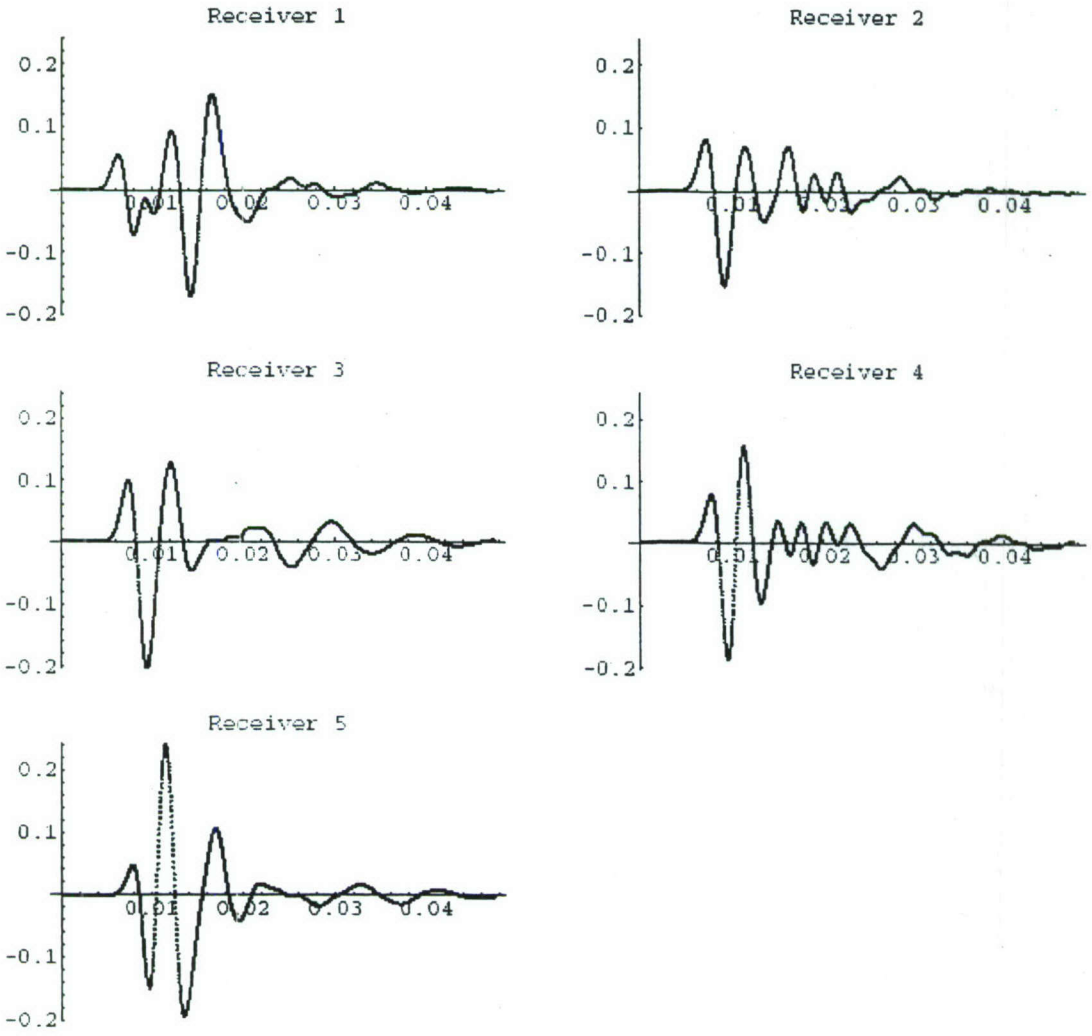

FIG. 10. Vertical components of the particle velocity at the five receiver locations with the mine beneath reconsolidated soil. Recall that Receivers 1 and 5 are the outermost and Receiver 3 is over the center of the mine.

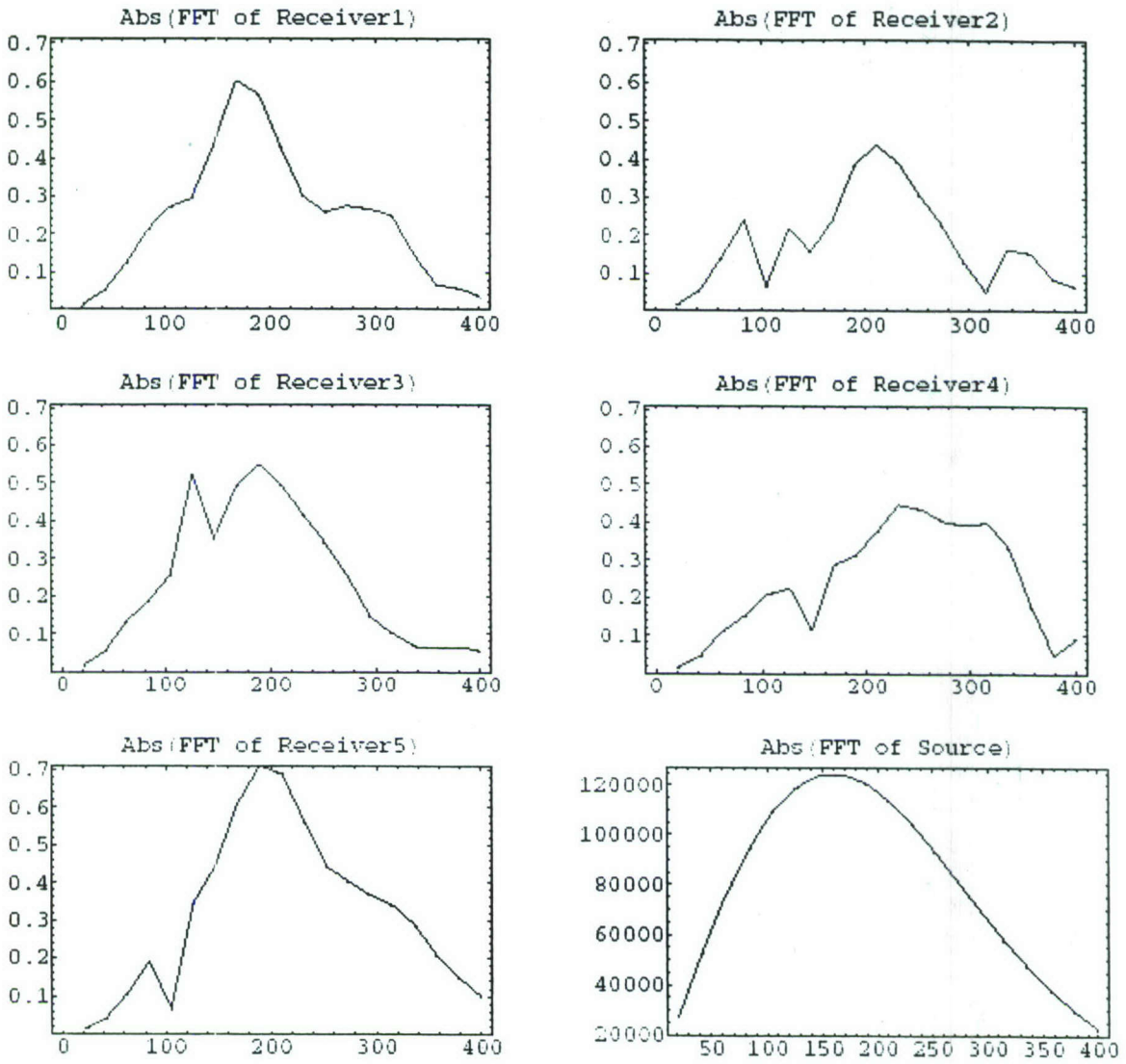

FIG. 11. Absolute values of the Fourier transforms of the receiver signals with a mine beneath reconsolidated soil, along with that of the source signal